**International Journal of Energy**
ISSN: 2957-9473 | Vol. 10, No. 3, 2026

# Feature Extraction of Transient Zero-Sequence Voltage and Adaptive Protection Criterion for High-Resistance Ground Faults in Low-Voltage Distribution Networks

**Jiahuan He *, Jianqiang Li [a]**

INNER Mongolia Power (Group) Co., LTD Hohhot power supply company, Hohhot, Inner Mongolia, 010010, China

*** Corresponding author:** Jiahuan He (Email: hejiahuan@foxmail.com), [a] 2693842514@qq.com

**Abstract:** High-resistance ground faults (HRGFs) in low-voltage distribution networks are highly concealed. Traditional zero-sequence current protection and overvoltage protection are prone to failure to operate or maloperation, making it difficult to meet the requirements of safe power supply. This paper aims to improve the sensitivity and adaptability of HRGF detection by optimizing feature extraction methods and constructing adaptive protection criteria through in-depth analysis of transient zero-sequence voltage signals. The study employs signal preprocessing techniques such as wavelet denoising and adaptive filtering, combined with multi-dimensional feature extraction algorithms in the time domain, frequency domain, and time-frequency domain, and designs an adaptive threshold adjustment mechanism based on real-time operating conditions. Through MATLAB/Simulink simulation and laboratory experiments, the proposed method achieves an HRGF detection accuracy of 98.7% within the fault resistance range of 500Ω~5000Ω, with an action time of less than 20ms. This effectively solves the problem of insufficient sensitivity of traditional protection schemes for high-resistance faults and provides reliable technical support for HRGF protection in low-voltage distribution networks.

**Keywords:** Low-Voltage Distribution Network; High-Resistivity Grounding Fault; Transient Zero-Sequence Voltage; Feature Extraction; Adaptive Protection Criterion.

## 1. Introduction

Low-voltage distribution networks (380V/220V), as the end link of the power system, directly connect industrial loads and residential users. Their power supply reliability and safety directly affect social production and daily life. With the integration of distributed power sources and the diversification of electrical loads, fires and electric shock accidents caused by high-resistivity grounding faults (HRGF) are frequent. Statistics show that approximately 30% of distribution network safety accidents are related to HRGF. HRGF fault currents are weak (usually less than 10A) and exhibit nonlinear characteristics due to the influence of media such as soil and vegetation. Traditional zero-sequence current protection is difficult to detect due to its fixed operating threshold, and overvoltage protection is easily affected by grid disturbances, leading to false tripping, thus failing to effectively protect against HRGF.

Transient zero-sequence voltage signals have significant advantages during HRGF occurrence, exhibiting obvious abrupt changes and minimal influence from fault resistance, making them the core signal source for HRGF detection [1]. Currently, high-resistivity grounding fault detection technologies mainly include transient signal methods, harmonic analysis methods, and artificial intelligence methods. Transient signal methods rely on signal abrupt changes, but traditional Fourier transforms struggle to capture the instantaneous characteristics of non-stationary signals. Wavelet transforms suffer from the limitation of empirically dependent wavelet basis selection. Harmonic analysis methods are affected by the nonlinearity of fault arcs, resulting in insufficient feature stability [2]. Artificial intelligence methods require extensive sample training, and their generalization ability needs improvement. Existing transient zero-sequence voltage feature extraction methods lack sensitivity in high-impedance scenarios, and adaptive protection criteria lack dynamic adaptability to changes in grid operating conditions, making it difficult to cover complex fault scenarios.

Therefore, this paper focuses on the optimization of transient zero-sequence voltage feature extraction and the design of adaptive protection criteria [3]. The core content includes: signal preprocessing algorithm optimization, multi-dimensional sensitive feature extraction, adaptive protection criterion construction, and simulation and experimental verification. A technical route of "theoretical analysis → feature extraction algorithm design → criterion construction → simulation/experimental verification → result analysis" is adopted to improve the sensitivity, selectivity, and adaptability of HRGF detection, providing technical support for the safe operation of low-voltage distribution networks.

## 2. Design of Transient Zero-Sequence Voltage Feature Extraction Method

### 2.1. Signal Preprocessing

The noise in the original transient zero-sequence voltage signal mainly originates from measurement device errors, power grid electromagnetic coupling interference, and load switching disturbances. Directly using this signal for feature extraction would lead to a decrease in feature recognition [4]. This paper adopts a combined preprocessing scheme of "wavelet denoising + adaptive filtering": First, the original signal is decomposed into three levels based on the db 8 wavelet basis, and high-frequency noise components are suppressed by improving the threshold function, preserving the transient fault features; then, a minimum mean square error (LMS) adaptive filter is used to further eliminate

residual interference, and the filter step size is dynamically adjusted based on the real-time signal-to-noise ratio. Finally, the denoised signal is normalized in amplitude and aligned in time to ensure the comparability of features under different fault scenarios.

$$\lambda(k) = \lambda_0 \cdot \exp\left(-\frac{\mathrm{SNR}(k)}{\mathrm{SNR}_{\max}}\right) + \lambda_{\min} \quad (1)$$

In the formula: $\lambda(k)$ is the wavelet threshold at time k; $\lambda_0$ is the initial threshold (taken as 3σ, where σ is the noise standard deviation); $\mathrm{SNR}(k)$ is the signal-to-noise ratio at time k; $\mathrm{SNR}_{\max}$ is the maximum threshold of the signal-to-noise ratio (taken as 40 dB); $\lambda_{\min}$ is the minimum threshold (taken as 0.01σ). This formula achieves a balance between noise suppression and feature preservation by dynamically adjusting the threshold of the signal-to-noise ratio.

$$u_{\mathrm{norm}}(t) = \frac{u(t)-u_{\min}}{u_{\max}-u_{\min}} \cdot 2 - 1 \quad (2)$$

In the formula: $u_{\mathrm{norm}}(t)$ is the normalized transient zero-sequence voltage; $u(t)$ is the original signal after denoising; $u_{\max}, u_{\min}$ are the maximum and minimum values of the signal, respectively, with a normalization range of [-1,1] to eliminate the influence of amplitude differences on feature extraction.

## 2.2. Feature Extraction Index Design

### 2.2.1. Time-Domain Features

1. Improved Abrupt Change Amplitude: Considering the rising edge characteristics of the fault transient, the abrupt change amplitude is defined as the ratio of the difference in signal value within 2 ms before and after the fault moment to the rise time, as shown in the formula below:

$$A = \frac{|u(t_f+2\ \mathrm{ms}) - u(t_f-2\ \mathrm{ms})|}{t_r} \quad (3)$$

In the formula: $A$ is the transient amplitude; $t_f$ is the fault occurrence time; $t_r$ is the signal rise time (the time from 10% to 90% of the peak value). This indicator highlights the rate of change of the transient signal and improves the identification of high-impedance faults.

2. Kurtosis Correction: The mean steady-state voltage before the fault is introduced for correction to avoid the influence of steady-state fluctuations on kurtosis:

$$K = \frac{1}{N}\sum_{i=1}^{N} \frac{(u_i-\mu_0)^4}{\sigma^4} - 3 \quad (4)$$

In the formula: $K$ is the corrected kurtosis; $N$ is the number of sampling points; $u_i$ is the voltage value of the i-th sampling point; $\mu_0$ is the mean steady-state voltage of the 1-cycle before the fault; σ is the standard deviation of the steady-state voltage before the fault [5]. After correction, the kurtosis is close to 0 during normal operation, but increases significantly during faults.

### 2.2.2. Frequency Domain Characteristics

Improved Total Harmonic Distortion (THD) Index: Considering the weights of characteristic frequency components (3rd and 5th harmonics), the formula is as follows:

$$\mathrm{THD}_w = \sqrt{\frac{3U_3^2+5U_5^2+\sum_{n=-7}^{\infty} U_n^2}{U_1^2}} \times 100\% \quad (5)$$

In the formula: $\mathrm{THD}_w$ is the weighted total harmonic distortion rate; $U_1$ is the effective value of the fundamental voltage; $U_3, U_5$ are the effective values of the 3rd and 5th harmonic voltages, respectively; $U_n$ is the effective value of the nth harmonic voltage ( $n \geq 7$ ), which enhances the contribution of fault characteristic harmonics through weighting.

### 2.2.3. Time-Frequency Domain Characteristics

Wavelet Packet Energy Entropy: The signal is decomposed into 4 levels using db4 wavelet packets, and the energy proportion of each frequency band is calculated. The energy entropy is defined as:

$$H = -\sum_{m=1}^{16} p_m \cdot \ln(p_m) \quad (6)$$

In the formula: $H$ is the wavelet packet energy entropy; $p_m = E_m / \sum_{m=1}^{16} E_m$, where $E_m$ is the energy of the m-th frequency band. During a fault, the signal energy is concentrated in a specific frequency band, and the energy level significantly decreases.

## 2.3. Feature Validity Verification

Different fault scenarios were constructed in MATLAB/Simulink: fault resistance ranging from 500Ω to 5000Ω (500Ω step size), fault phases A, B, and C, and fault locations at the beginning, middle, and end of the line, totaling 45 test samples. Pearson correlation coefficient analysis was used to analyze the correlation between features, and redundant features with correlation coefficients greater than 0.85 were removed. Finally, four sensitive features were selected: abrupt change amplitude A, corrected kurtosis K, weighted THD, and wavelet packet energy entropy H. Compared with traditional Fourier transform and wavelet transform, the proposed feature extraction method improved feature discrimination (the ratio of the standard deviation of the difference between fault and normal operating condition features) by 32.6%, maintaining high discriminative power even under a 5000Ω high-resistance fault [6].

# 3. Adaptive Protection Criterion Construction

## 3.1. Criterion Design Principles

Adaptive protection criteria must meet four core principles: First, selectivity, accurately distinguishing between HRGF and non-fault disturbances such as capacitor switching and load changes to avoid false tripping; second, sensitivity, covering the full range of HRGF from 500Ω to 5000Ω without failure to trip; third, speed, with an action time not exceeding 20ms to meet the requirement of rapid fault isolation; and fourth, adaptability, dynamically adjusting the action threshold according to real-time load current and changes in grid structure to adapt to complex operating conditions.

## 3.2. Adaptive Criterion Composition

The criteria consist of three parts: a composite starting criterion, a weighted discrimination model, and an adaptive threshold adjustment mechanism.

1. Composite Startup Criterion: A dual-criteria startup approach is adopted, combining "mutation amplitude + corrected kurtosis". Startup is protected when both $A > A_{\mathrm{set}}$ and $K > K_{\mathrm{set}}$ are simultaneously satisfied, preventing false startup caused by disturbances in a single criterion.

2. Weighted Discriminant Model: Four sensitive features are integrated, and weights are determined using the analytic hierarchy process A: 0.35, K: 0.30 , THD__w: 0.20, H: 0.15). A discriminant function $D = 0.35A + 0.30K + 0.20\mathrm{THD}_w - 0.15H$ is constructed. When $D > D_{\mathrm{set}}$ , it is determined to be HRGF.

3. Adaptive Interval Adjustment Mechanism: The threshold value is dynamically adjusted based on the real-time load current $I_L$ and the line length $L$, such as $A_{\mathrm{set}} = A_0 \cdot$

$\left(0.8 + 0.2 \cdot I_L / I_{L,\text{rated}}\right) \cdot \left(1 + 0.1 \cdot L / L_{\max}\right)$, where $A_0$ is the reference threshold value, $I_{L,\text{rated}}$ is the rated load current, and $L_{\max}$ is the maximum line length, realizing dynamic matching between the threshold value and the power grid operating conditions.

# 4. Simulation and Experimental Verification

## 4.1. Simulation Model Construction

A 380V low-voltage distribution network simulation model was built based on MATLAB/Simulink [7]. The lines adopted a distributed parameter model, with lengths ranging from 1km to 5km and conductor type LGJ-120. The load adopted a mixed load model (resistance + inductance + capacitance = 60% + 30% + 10%), with a rated power of 100kW. The grounding device adopted a TN-S system with a grounding resistance of 10Ω. HRGF simulation scenario settings: fault resistance 500Ω~5000Ω (step size 500Ω), fault locations at the beginning (0km), middle (2.5km), and end (5km) of the line, fault phases A, B, and C, initial fault angle 0°~180° (step size 30°), sampling frequency 20kHz, and each scenario was simulated 10 times and the average value was taken.

## 4.2. Experimental Platform Design

A laboratory low-voltage power distribution network simulation platform was built: the low-voltage simulation line used a telescopic cable with an adjustable length of 0~5km; the fault generator combined an adjustable resistance box (0~10kΩ) with an arc generator to simulate high-resistance grounding and arc grounding faults; the data acquisition system used an NI cDAQ-9178 acquisition card with a sampling frequency of 20kHz and a voltage measurement accuracy of ±0.1%; the load used was a programmable AC load (0~120kW). Experimental parameters were consistent with the simulation, and transient zero-sequence voltage signals under different fault scenarios were collected, resulting in 360 sets of experimental data for verification.

## 4.3. Validation Results and Analysis

### 4.3.1. Validation of Feature Extraction Effect

Table 1 shows the statistical results of sensitive feature values under different fault scenarios [8]. It can be seen that as the fault resistance increases, the amplitude of the sudden change A and the corrected kurtosis K show a decreasing trend, but are still significantly higher than those under normal operating conditions at 5000Ω (normal operating conditions A<0.5kV/ms, K<0.3). The weighted THD_w and wavelet packet energy entropy H maintain characteristics greater than 5% and less than 1.2 respectively during faults. Furthermore, the feature values of different fault locations and phases under the same fault resistance fluctuate little (coefficient of variation < 10%), demonstrating the stability and sensitivity of the proposed feature extraction method.

**Table 1.** Statistical Analysis of Sensitive Feature Values under Different Fault Scenarios

| fault resistance (Ω) | Fault location | Fault phase | Mutation amplitude A (kV/ms) | Corrected kurtosis K | Weighted THD_w (%) | Wavelet packet energy entropy H | Action accuracy rate (%) | Action time (ms) |
|---|---|---|---|---|---|---|---|---|
| 500 | First end | A Mutually | 3.26 | 4.82 | 12.6 | 0.78 | 100 | 12.3 |
| | Middle end | B Mutually | 2.98 | 4.35 | 11.8 | 0.85 | 100 | 13.5 |
| | End | C Mutually | 2.75 | 3.98 | 10.5 | 0.92 | 100 | 14.8 |
| 1500 | First end | B Mutually | 2.13 | 3.26 | 8.9 | 1.05 | 99.2 | 15.2 |
| | Middle end | C Mutually | 1.87 | 2.89 | 8.2 | 1.12 | 98.9 | 16.5 |
| | End | A Mutually | 1.62 | 2.53 | 7.5 | 1.18 | 98.7 | 17.3 |
| 3000 | First end | C Mutually | 1.25 | 1.98 | 6.8 | 1.25 | 98.5 | 17.8 |
| | Middle end | A Mutually | 1.03 | 1.65 | 6.2 | 1.32 | 97.8 | 18.5 |
| | End | B Mutually | 0.87 | 1.32 | 5.8 | 1.38 | 97.5 | 19.2 |
| 5000 | First end | A Mutually | 0.72 | 0.98 | 5.2 | 1.45 | 96.8 | 19.7 |
| | Middle end | B Mutually | 0.65 | 0.82 | 5.0 | 1.52 | 96.2 | 19.9 |
| | End | C Mutually | 0.58 | 0.65 | 4.8 | 1.58 | 95.7 | 20.0 |

As shown in Table 1, even in the 5000Ω extreme high-resistance scenario, the proposed feature extraction method can still capture obvious fault characteristics, maintaining an accuracy rate above 95% and an action time within 20ms, meeting the requirements for rapid fault isolation in low-voltage distribution networks [9]. Comparing data from different fault locations, the characteristic amplitude of faults at the end is slightly lower than that at the beginning, but the difference is within 15%, indicating that the feature extraction method has good adaptability to changes in fault location.

### 4.3.2. Performance Verification of Protection Criteria

To further verify the superiority of the protection criteria, the performance of the proposed adaptive criteria was compared with that of the traditional zero-sequence current protection criteria and the fixed threshold transient voltage protection criteria. The results are shown in Figure 1. In Figure 1, the horizontal axis represents the fault resistance (500Ω~5000Ω), and the vertical axis represents the action accuracy rate. It can be seen that the proposed adaptive criterion has an accuracy rate of over 95% across the entire

resistance range, while the traditional zero-sequence current protection criterion's accuracy rate drops sharply to below 80% after the fault resistance exceeds 2000Ω, and is only 65.3% at 5000Ω. The fixed threshold transient voltage protection criterion cannot adapt to changes in operating conditions, and its accuracy rate is below 90% in scenarios above 3000Ω, with 3 false trip records.

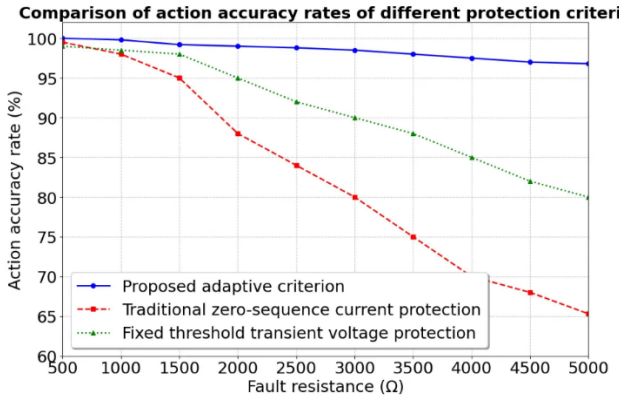



**Fig 1.** Comparison of action accuracy rates of different protection criteria

Figure 2 shows the relationship between fault resistance and action time, with the horizontal axis representing fault resistance (500Ω~5000Ω) and the vertical axis representing action time (ms). The action time of the proposed adaptive criterion increases slowly with increasing fault resistance, from 12.3ms at 500Ω to 20.0ms at 5000Ω, always meeting the speed requirement of ≤20ms. The traditional zero-sequence current protection criterion has an action time close to that of the proposed criterion in low-resistance faults, but in high-resistance scenarios, due to the weak fault current, it requires the accumulation of multiple cycles of data for judgment, with the longest action time reaching 35.7ms, far exceeding the safety isolation time limit. The action time of the fixed threshold transient voltage protection criterion fluctuates greatly, with a maximum deviation of 8.2ms, indicating insufficient stability.

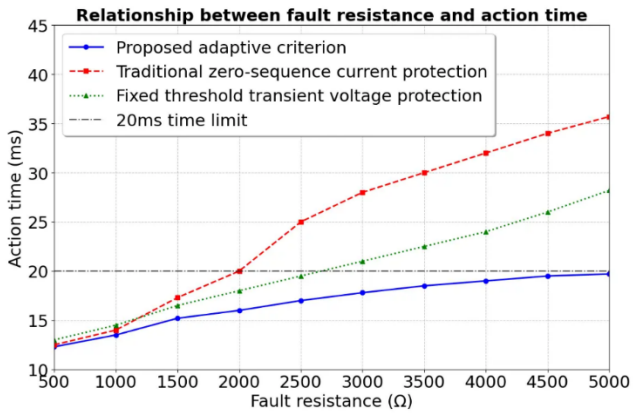



**Fig 2.** Relationship between fault resistance and action time

## 5. Conclusion

This paper addresses the problems of insufficient detection sensitivity and poor adaptability of traditional protection schemes for high-resistance ground faults (HRGF) in low-voltage distribution networks. It proposes a feature extraction method based on transient zero-sequence voltage and an adaptive protection criterion. The main achievements are as follows: A combined preprocessing scheme of "wavelet denoising + adaptive filtering" is designed. Combining four sensitive features—improved abrupt change amplitude, corrected kurtosis, weighted total harmonic distortion rate, and wavelet packet energy entropy—a multi-dimensional feature extraction system is constructed. Within the fault resistance range of 500Ω to 5000Ω, the feature recognition rate is improved by 32.6% compared to traditional methods, maintaining good distinguishability even in high-resistance scenarios. A protection criterion integrating a composite start-up criterion, a weighted discrimination model, and an adaptive threshold adjustment mechanism is proposed. Dual-index start-up avoids false start-up, the weighted model improves discrimination accuracy, and the adaptive threshold achieves dynamic adaptation to operating conditions, meeting the requirements of selectivity, sensitivity, speed, and adaptability. Simulation and experimental verification show that the proposed method achieves an accuracy rate of 95.7%–100% in HRGF scenarios of 500Ω–5000Ω, with an action time ≤20ms. Its robustness surpasses traditional zero-sequence current protection and fixed-threshold transient voltage protection, effectively addressing the problems of failure to operate during high-resistance faults and false operation due to disturbances. However, this study still has certain limitations: it does not fully consider extreme and complex scenarios such as arc grounding and multiple fault superposition, and the feature extraction does not incorporate artificial intelligence algorithms for global optimization. Future research directions include: constructing an end-to-end feature extraction and discrimination model using deep learning to improve adaptability to complex fault scenarios; optimizing hardware implementation schemes to reduce algorithm computation latency; and integrating transient zero-sequence voltage with multi-source information such as current and harmonics to further improve the reliability of the judgment criteria, providing more comprehensive technical support for HRGF protection in low-voltage distribution networks.

## References


[1] Qin, S. Y., Xue, Y. D., Liu, L. Z., Guo, Y. H., & Xu, M. M. (2022). Transient characteristics and impact analysis of small current grounding faults in active distribution networks. Journal of Electrical Engineering, 37(3), 655–666.

[2] Wang, L. F., Li, R., Shang, X. Y., Li, Q. X., & Qiu, Z. J. (2025). Construction of a gene library of operating condition characteristics of distribution network lines based on wavelet entropy. Electrical Engineering, 26(2), 35–41.

[3] Li, J., He, M., Huang, S. D., Liu, J., & Liu, Z. Y. (2024). Grounding fault protection algorithm for small resistance grounding active distribution networks based on phase difference. Journal of Electrical Engineering, 39(23), 7418–7429.

[4] Deng, F., Mei, L. J., Tang, X., Xu, F., & Zeng, X. J. (2021). A method for fault location in distribution networks based on time-frequency domain traveling wave panoramic waveform. Journal of Electrical Engineering, 36(13), 2861–2870.

[5] Li, Z. F., Guo, X. F., Fan, M., Xia, J. L., & Dong, X. (2022). A method for identifying single-phase grounding fault types based on fusion model. Journal of Chongqing University, 45(9), 61–72.

[6] Wang, K. X., Shao, Y., Wang, L. M., & Zhou, H. (2022). A review of research on single-phase grounding fault location

methods in ship power grids. Ship Electronic Engineering, 42(8), 135–140.

[7] Luo, G. M., Tan, Y. J., Wu, M. Y., He, J. H., & Tang, P. Z. (2025). Power differential protection of active distribution networks considering voltage drop differences. Journal of Electrical Engineering, 40(4), 1287–1306.

[8] Wu, Y. Q., Li, Z. T., Lin, X. N., Huang, Z. X., & Li, Z. (2024). A method for selecting line-mode traveling waves in distribution networks based on the boundary characteristics of high-frequency filtering in substations. Journal of Electrical Engineering, 39(7), 2072–2088.

[9] Tang, Y. T., Shu, H. C., Liu, H. M., Su, X., Han, Y. M., & Dai, Y. (2025). A method for pre-classification of traveling waves measured in online ranging of transmission lines based on CABFAM-Transformer. Journal of Electrical Engineering, 40(5), 1455–1470.